Wave Motion ▮ (▮▮▮▮) ▮▮▮–▮▮▮

Contents lists available at ScienceDirect

Wave Motion

journal homepage: www.elsevier.com/locate/wamot

Extraction of the coupling impedance in overmoded cavities

Bisrat Addissie, John Rodgers, Thomas Antonsen *

University of Maryland, College Park, MD, United States

HIGHLIGHTS

- The radiation impedance is a key parameter in characterizing an antenna, and also particularly important in a statistical model of coupling to an overmoded cavity.
- Previous methods of measuring the radiation impedance present challenges that can be overcome by applying a time gating method.
- The time gating method presented here allows one to obtain the radiation impedance from a frequency domain measurement of the reflection coefficient in situ.
- It has the flexibility of including the effects of internal reflections in the cavity by adjusting the time gating parameters.
- The method is applied to the random coupling model and is successfully shown to agree with its theoretical predictions.

ARTICLE INFO

Article history:
Received 18 December 2017
Received in revised form 27 July 2018
Accepted 10 September 2018
Available online xxxx

Keywords:
Random coupling model
Time-gating method
Short orbits
Antenna characteristics

ABSTRACT

The radiation impedance is a key parameter in characterizing an antenna, and also particularly important in a statistical model of coupling to an overmoded cavity. Previous methods of measuring the radiation impedance present challenges that can be overcome by applying a time gating method. The time gating method presented here allows one to obtain the radiation impedance from a frequency domain measurement of the reflection coefficient in situ. It has the flexibility of including the effects of internal reflections in the cavity by adjusting the time gating parameters. The method is applied to the random coupling model and is successfully shown to agree with its theoretical predictions.

1. Introduction

The coupling of electromagnetic field energy into and out of enclosures such as electronics cases, rooms and compartments, and reverberation chambers depends sensitively on the details of the enclosure's geometry and on the frequency of the injected radiation. Because of this sensitive dependence, a statistical description of the system's response is often sought [1]. The random coupling model (RCM) introduced for electromagnetic problems [2–5] and reviewed recently [6,7] has been successfully demonstrated to describe the statistics of a system's impedance matrix relating the currents and voltages at identified ports. The RCM is based on previous work in the theoretical physics literature [8–10].

There are certain assumptions that need to be met for the RCM to apply. The first assumption is that the enclosure is electrically large. In other words, the wavelength of interest must be sufficiently small such that the port excites many modes in the cavity. Only then can a statistical approach such as the RCM be considered. Second, the enclosure must have ray chaotic dynamics. This means that in the small wavelength limit, where the launched waves in the enclosure can be thought of as rays, the dynamics are chaotic. By "chaotic" we mean to say that if two rays are launched with a very small difference in the launch angle or location the trajectories diverge from one another exponentially. Typically, this requires the rays to multiple

* Corresponding author.
E-mail address: antonsen@umd.edu (T. Antonsen).

https://doi.org/10.1016/j.wavemoti.2018.09.011
0165-2125/

strike curved surfaces. These assumptions ensure that the field distributions in the enclosure have the local character of a random superposition of plane waves and that the resonant frequencies have a characteristic distribution described by random matrix theory [11]. The third assumption and the topic of this paper is that the conditions of the ports are known and can be treated deterministically. The random nature of the system dynamics arises from the random scattering of rays in the enclosure itself, but not the ports. For all the ports, either their exact geometry and material properties are known such that the impedance of the ports under anechoic conditions can be computed numerically or, more practically, the impedance can be measured.

In the RCM, the impedance of the port under anechoic condition is called the radiation impedance (Z_{rad}). This is the impedance that would be measured at the port if there were no reflection from the enclosure's distant internal boundaries. The random coupling model allows one to statistically characterize electromagnetic energy coupled from one port to another; and in the simplest case from one port back to itself. According to the RCM, the values of the impedance that are measured at a port of a cavity can be modeled by the random variable

$$Z_{cav} = R_{rad}\xi + jX_{rad}, \tag{1}$$

where R_{rad} and X_{rad} are the real and imaginary part of the radiation impedance; and ξ is a complex random variable obtained from random matrix theory whose statistical properties are fully characterized by a single loss parameter. The loss parameter is essentially the average Q-width of resonant modes in the cavity normalized to the average spacing between modes. The dependence of ξ on this loss parameter is described in Ref. [3]. In the lossless case it is purely imaginary and Lorentzian distributed. As loss increases, the real part of ξ approaches unity with small Gaussian fluctuations, and the imaginary part of ξ approaches zero with small independent Gaussian fluctuations. Thus, in this limit the cavity impedance approaches the radiation impedance. Eq. (1) applies to the case of a single port and determines a scalar impedance. For a cavity with multiple ports [4] there is a simple matrix generalization of Eq. (1) in which the quantities are matrices and the first term is written $\boldsymbol{R_{rad}}^{1/2}\,\boldsymbol{\xi}\boldsymbol{R_{rad}}^{1/2}$.

There have been two methods suggested to measure the radiation impedance. The first method is to line the enclosure walls with radiation absorbing material, and is the method used by Hemmady et al. [5]. in experiments to validate the RCM. This method can be time consuming and requires access to the interior of the enclosure. Furthermore, this method requires assigning to the port a portion of the wall of the enclosure in proximity to the port. This boundary where a port ends and the enclosure begins may be difficult to determine. The other method is to use a mode stirrer inside the enclosure and collect an ensemble of impedance measurements. The average of a large ensemble of measurements will converge to the radiation impedance. This requires that the mode stirrer sufficiently mixes the modes in the enclosure and that a large enough ensemble is sampled; both of which are difficult to realize in practical enclosures. On the other hand, the time gating method described in the following sections only requires a single measurement at the port. Access to the interior of the enclosure is not required. The characteristic reflections from the nearby enclosure walls can be adjusted by a single parameter: the gating time. The implementation of the time gating method will be discussed in this paper. The paper is organized as follows. The time gating method and its implementation to measure the RCM parameters are described in Sections 2 and 3. Results from experimental validation of the method are presented in Section 4. A discussion of the potential sources of error in time gating and solutions including a treatment of the localized power loss at the port are presented in Section 5. Finally, the main ideas are summarized in Section 6.

2. Time gating method

Time-gating is a method by which a frequency domain measurement is effectively averaged over a sliding window in the frequency domain. The method applies the Fourier transform of the measured complex reflection coefficient to the time domain, gating it in time, and Fourier transforming back to the frequency domain. If T_G is the duration of gating, then T_G^{-1} is the effective width of the frequency window. The purpose of the time gating presented here is the determination of the radiation impedance of the port including the effect of reflections from objects in the near field and excluding the effect of multiple far field reflections.

Time gating has been used for decades to improve frequency domain measurements [12]. In an antenna pattern measurement, the time-gating method (TGM) is used to remove unwanted multipath reflections from structures near the antenna [13,14]. Ideally an antenna pattern is measured in an anechoic chamber where reflections from the walls are suppressed by radiation absorbing material. However, if an anechoic chamber is not available, or if the absorbers are not well suited for the frequency range of interest, there will be unwanted reflections from the walls. This is where the TGM can be used to suppress the reflections from the walls. In addition to this, it is also used to characterize reverberant chambers [15]. In this case, the information that characterizes the reverberant chamber is found in the difference between the ungated and the time gated measurement. In these cases, the TGM has been a valuable tool.

The TGM is implemented in some modern vector network analyzers (VNA). In a VNA, the reflection coefficient is measured in the frequency domain using a swept CW source and a receiver that tracks the amplitude and the phase of the received signal. The TGM method process is shown in Eq. (2),

$$\begin{aligned} &\bar{S}(f) \xrightarrow{\mathcal{F}^{-1}} s(t) \\ &s(t)\,g(t) \xrightarrow{\mathcal{F}} \bar{S}_g(f)\,. \end{aligned} \tag{2}$$

Please cite this article in press as: B. Addissie, et al., Extraction of the coupling impedance in overmoded cavities, Wave Motion (2018), https://doi.org/10.1016/j.wavemoti.2018.09.011.

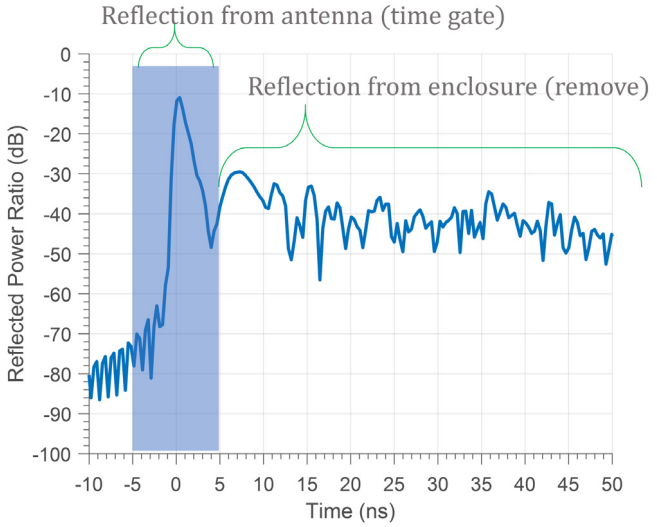

Fig. 1. A power delay profile obtained by Fourier transforming the reflection coefficient of the antenna radiating inside a reverberant enclosure. The first peak comes from the antenna and subsequent peaks are reflections from the enclosure walls.

The complex reflection coefficient $\bar{S}(f)$ is transformed to the time domain using an inverse fast Fourier transform (IFFT). This time domain signal $s(t)$ is multiplied by a gating window function $g(t)$ to select the duration of the time window of interest and suppress the rest. The gated time domain signal is Fourier transformed back to the frequency domain to arrive at the desired result $\bar{S_g}(f)$.

Another way to implement the TGM, is to use the fact that multiplication in the time domain is equivalent to a convolution in the frequency domain. The time domain gating window is transformed to the frequency domain using a fast Fourier transform (FFT) and convolved with the raw frequency domain measurement. The result is the gated reflection coefficient. This can be expressed as,

$$\bar{S_g}(f) = \bar{S}(f) \otimes \bar{G}(f), \tag{3}$$

where $\bar{S}(f)$ is the unprocessed frequency domain S-parameter measurement, $g(t)$ is the gating function in time and $\bar{G}(f)$ is its Fourier transform, and $\otimes$ is the convolution operator.

One of the advantages of the TGM is the flexibility in being able to choose a gating time and gating function to include the effect of prominent reflections. After collecting reflection coefficient data over the frequency range of interest, we Fourier transform the data into the time domain. A plot of the time domain data allows us to visualize the dominant reflections along the signal path. For example, results of a measurement of the reflection coefficient from an antenna radiating into a cavity are shown in Fig. 1. In this example, an L-band helical antenna irradiates a 3 m^3 aluminum cavity. We can see that there is a clear prompt reflection from the antenna centered at $t = 0$ [ns]. This prompt reflection gives us valuable information about the port; namely, how much power enters the cavity.

If we set the gating time to include only this peak, and transform back to the frequency domain, we obtain a reflection coefficient that is window-averaged over a broad frequency range. This window average eliminates important structure in the reflection coefficient associated with reflections from nearby walls [16,17] . Returning to the time domain, Fig. 1, for some time after the prompt reflection, $t > 5$ ns, there are many strong temporal peaks or reflections from the cavity that give rise to systematic variations of the reflection coefficient with frequency. When measuring the radiation impedance (associated with prompt reflection), these later reflections are removed: for this example, we might choose a gating time to be 5 ns, however, if we desire to average over a smaller frequency range, and thus include multiple reflections from the nearby walls, we can do so by further increasing the gating time. This is addressed in Section 3. Once we have decided on the gating time, we need to select a gating function. If we use a rectangular windowing function in time, then in the frequency domain the measurement is convolved with a sinc-function, which has alternating positive and negative lobes. If we use a Gaussian window, then the windowing function is a Gaussian and is always positive. For simplicity, we will use a rectangular function in this paper such that the gating is given by,

$$g(t) = \begin{cases} 1 & : t < T_G \\ 0 & : t \geq T_G \end{cases} \tag{4}$$

where T_G is the gating time.

Please cite this article in press as: B. Addissie, et al., Extraction of the coupling impedance in overmoded cavities, Wave Motion (2018), https://doi.org/10.1016/j.wavemoti.2018.09.011.

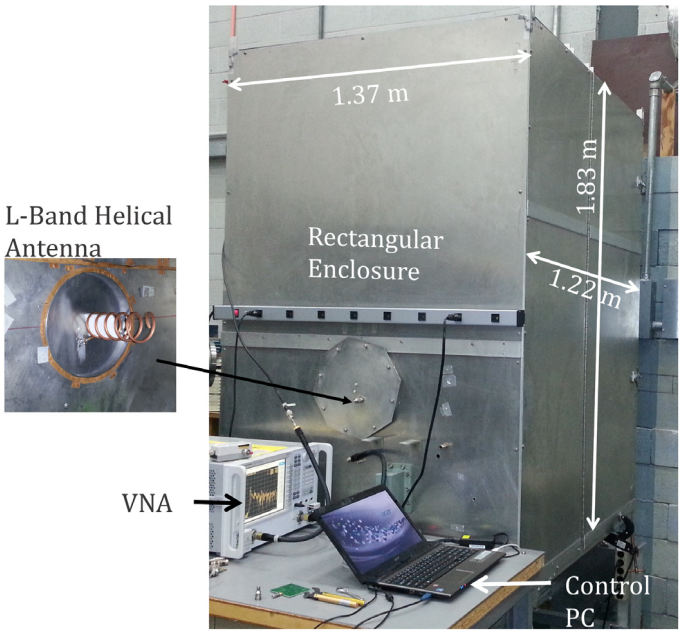

Fig. 2. The measurement setup showing the rectangular enclosure, the VNA to make the measurements, and the control PC to collect and analyze the measurements.

3. Determination of Z_{rad} using TGM

We illustrate the time gating method by considering a particular antenna. We measure the impedance of an L-band helical antenna in a mode stirred rectangular reverberant chamber shown in Fig. 2. This aluminum enclosure has dimensions 1.37 m x 1.22 m x 1.83 m for a volume of 3.06 cubic meters. The helical antenna is made from quarter inch copper tube, 24.1 cm in length. The measurement is taken over the frequency range of 1.5 GHz to 3.5 GHz, over which the RCM loss parameter (α) is measured to be 2.8. The quantity α, the only parameter required to fully characterize ξ in Eq. (1) [6], is given by

$$\alpha = \frac{\omega}{2\Delta\omega Q} \tag{5}$$

where ω, Q, $\Delta\omega$ are the angular frequency and the quality factor and the average mode spacing, respectively. The quality factor is measured from the energy decay time constant (τ) for the enclosure from which

$$Q = \omega\tau. \tag{6}$$

The energy decay time constant is obtained by Fourier transforming the measured reflection coefficient (S_{11}) to the time domain ($h_{11}(t)$), then squaring the result. The squared result is referred to as the power delay profile (PDP) as shown in Eq. (7),

$$PDP = |h_{11}(t)|^2. \tag{7}$$

The power delay profile from a single measurement as function of time is shown in Fig. 3. The slope is computed during the 1 μs - 4 μs period by smoothing average of the power delay profile. The slope (-ν [dB/s]) is then used to compute time constant quantity factor which in this case is measured to be 7980,

$$\tau = 4.34/\nu. \tag{8}$$

The mean mode spacing, on the other hand, is determined theoretically using Weyl's formula [18] given by

$$\Delta\omega = \frac{\pi^2 c^3}{\omega^2 V}, \tag{9}$$

where c and V are the speed of light and the volume of the cavity, respectively. The mode stirrer consists of a sheet of aluminum held at a 45 degree angle on shaft that is rotated by a programmable stepper motor. We generate 50 cavity

Please cite this article in press as: B. Addissie, et al., Extraction of the coupling impedance in overmoded cavities, Wave Motion (2018), https://doi.org/10.1016/j.wavemoti.2018.09.011.

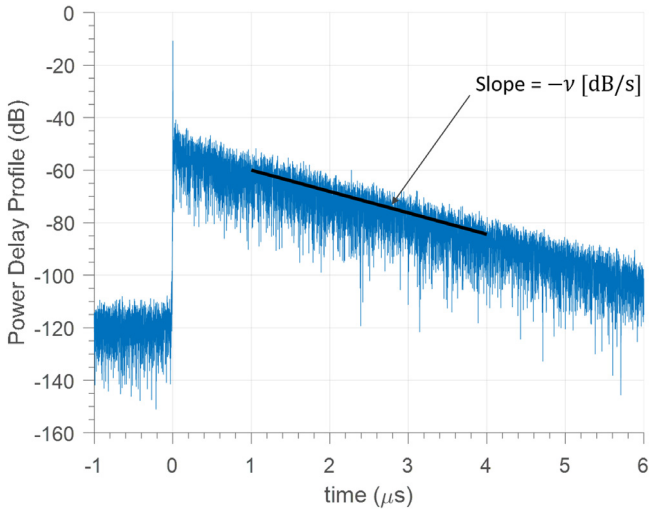

Fig. 3. The power delay profile computed by Fourier transforming the reflection coefficient. The slope is used to compute the energy decay time constant (τ).

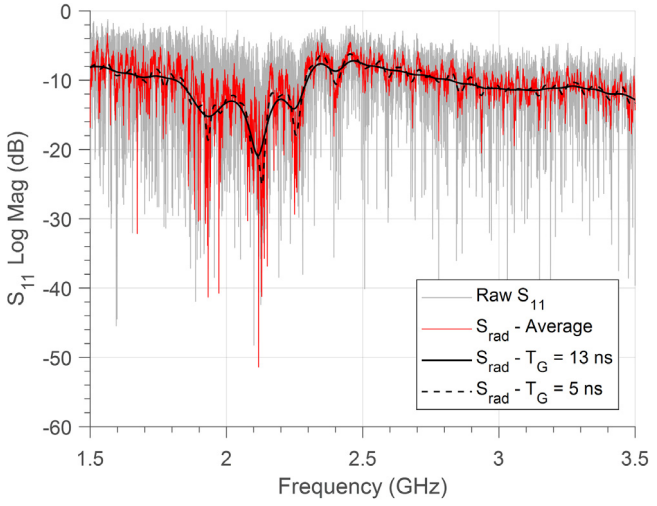

Fig. 4. The radiation scattering parameter (S_{rad}) approximated by the following three methods: red—averaging over an ensemble of 50 cavity realization obtained by rotating the stirrer, black obtained from TGM (solid $T_G = 5$ ns, dashed $T_G = 13$ ns). In gray is S_{11} measured for a single cavity realization . (For interpretation of the references to color in this figure legend, the reader is referred to the web version of this article.)

realizations for 50 distinct positions of the mode stirrer. Fig. 4 displays three versions of the magnitude of the reflection coefficient, $|S_{11}|$. Shown in light gray is the reflection coefficient obtained from one position of the stirrer. Shown in red is the average reflection coefficient obtained by averaging $|S_{11}|$ over the 50 stirrer positions. The black solid curves and the black dashed line are the reflection coefficients obtained using the TGM as follows.

To obtain the window averaged reflection coefficient using TGM one must select a gating time. The effect of varying the gating time is to include or exclude contributions to the reflection coefficient from the ray paths or orbits that leave the antenna, bounce off a wall, and return. The effect of the orbits is specific to the cavity under consideration and not included in the model impedance, Eq. (1). The treatment of the orbits, called short orbits was addressed theoretically by Hart et al. [17] and implemented by Yeh et al. [16]. The approach is to replace Z_{rad} in Eq. (1) by Z_{avg} where Z_{avg} is a frequency window average of the raw impedance matrix. In principle, there are mathematical formulas for Z_{avg} involving summations of contributions from a small number of ray paths [16,17]. To do this using TGM we look at the power delay profile in Fig. 1. We set the delay window time to $T_G = 13$ ns and inverse Fourier transform to obtain the TGM reflection coefficient shown as the dashed curve in Fig. 4. For comparison, the reflection coefficient using a windowing time of $T_G = 5$ ns is also shown in Fig. 4. The reflection coefficient has significantly less structure in frequency that either the ensemble average reflection coefficient or

Please cite this article in press as: B. Addissie, et al., Extraction of the coupling impedance in overmoded cavities, Wave Motion (2018), https://doi.org/10.1016/j.wavemoti.2018.09.011.

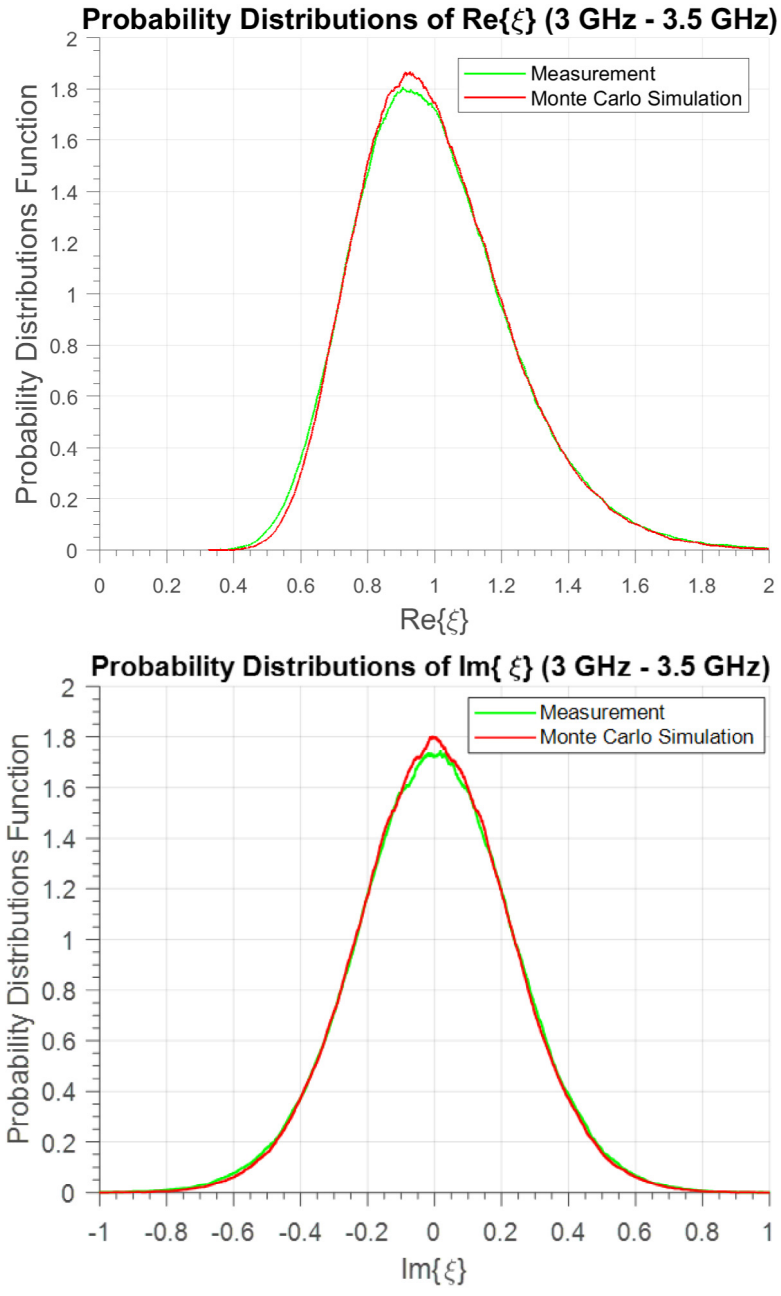

Fig. 5. A comparison of the real (top) and imaginary (bottom) part of the measured and computed normalized impedances over the frequency range 3 GHz 3.5 GHz.

the TGM, $T_G = 13$ ns reflection coefficient. This will be of significance when we characterize fluctuations about the average impedance in the next section.

4. Impedance fluctuations

We measure frequency scans of the reflection coefficient for 50 positions of the stirrer. In addition, we apply TGM to one of these scans using Eq. (3) with two different gating times, $T_G = 5$ ns and $T_G = 13$ ns. We convert these frequency dependent reflection coefficients to the frequency dependent impedances using,

$$\frac{Z_{cav}}{Z_0} = \frac{1 + S_{11}}{1 - S_{11}} \tag{10}$$

Please cite this article in press as: B. Addissie, et al., Extraction of the coupling impedance in overmoded cavities, Wave Motion (2018), https://doi.org/10.1016/j.wavemoti.2018.09.011.

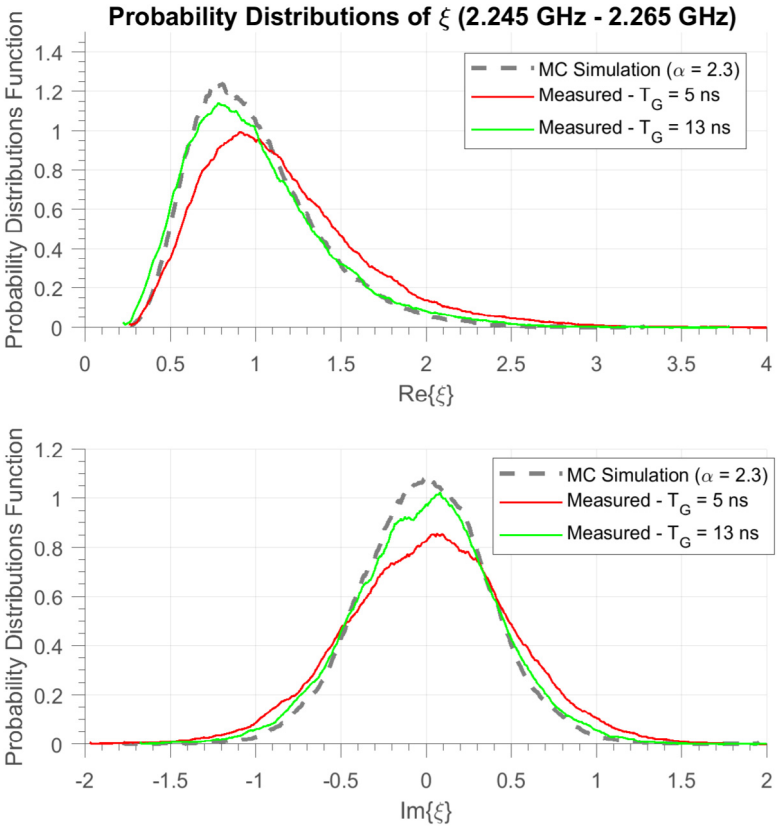

Fig. 6. A comparison of the pdfs of the real (top) and imaginary (bottom) part of the measured and computed normalized impedances over the frequency range 2.245 GHz -2.265 GHz where the short orbits have a stronger effect of the pdfs.

where $Z_0 = 50\ \Omega$ is the characteristic impedance of the transmission line feeding the antenna. We then "normalize" the measured values of the impedance using the formula implied by Eq. (1),

$$\xi_m = \frac{Z_{cav} - j\bar{X}}{\bar{R}}, \tag{11}$$

where Z_{cav} are the raw measurement of the input impedance at the port and $\bar{Z} = \bar{R} + j\bar{X}$ is either the radiation impedance Z_{rad} ($T_G = 5$ ns) or the TGM determined impedance Z_{avg} ($T_G = 13$ ns).

According to the RCM the values of ξ_m should behave as random variables with a probability density function that depends on the loss parameter (α), which is measured, by the method discussed in Section 3, to be 6 for the frequency range of 3 GHz to 3.5 GHz. The quantity ξ_m is computed from the measured Z_{cav} and normalized by Z_{rad} ($T_G = 5$ ns). We compare the distribution of ξ_m with the RCM prediction. The predicted distribution is obtained from the Monte Carlo simulation described in Appendix A of [6]. The two distributions of the real and imaginary part of the normalized impedance (ξ) are good agreement as shown in Fig. 5.

Over the frequency range 2.245 GHz and 2.265, The loss parameter α is 2.3. In this 20 MHz window, as shown in Fig. 6, there is a significant difference between the radiation impedance and the TGM acquired impedance with $T_G = 13$ ns. This will affect the distribution of ξ_m as given by Eq. (11). Three pdfs of the real and imaginary part ξ_m using Eq. (11) are shown in Fig. 6. The pdf that is in best agreement with the predicted pdf is obtained from ξ_m that is normalized with the TGM determined impedance using a time window that includes short orbits ($T_G = 13$ ns). The agreement with its prediction is better than the impedance normalized with the radiation impedance ($T_G = 5$ ns). These results confirm the RCM statistical model can be applied provided that the appropriate average impedance is used in Eq. (11) to "normalize" the measured values of cavity impedance.

5. Discussion

The results of the previous section show that the measured values of the cavity impedance can be modeled by the RCM provided the appropriate values of the average impedance $\bar{Z} = \bar{R} + j\bar{X}$ is used in Eq. (11). This value of average impedance

Please cite this article in press as: B. Addissie, et al., Extraction of the coupling impedance in overmoded cavities, Wave Motion (2018), https://doi.org/10.1016/j.wavemoti.2018.09.011.

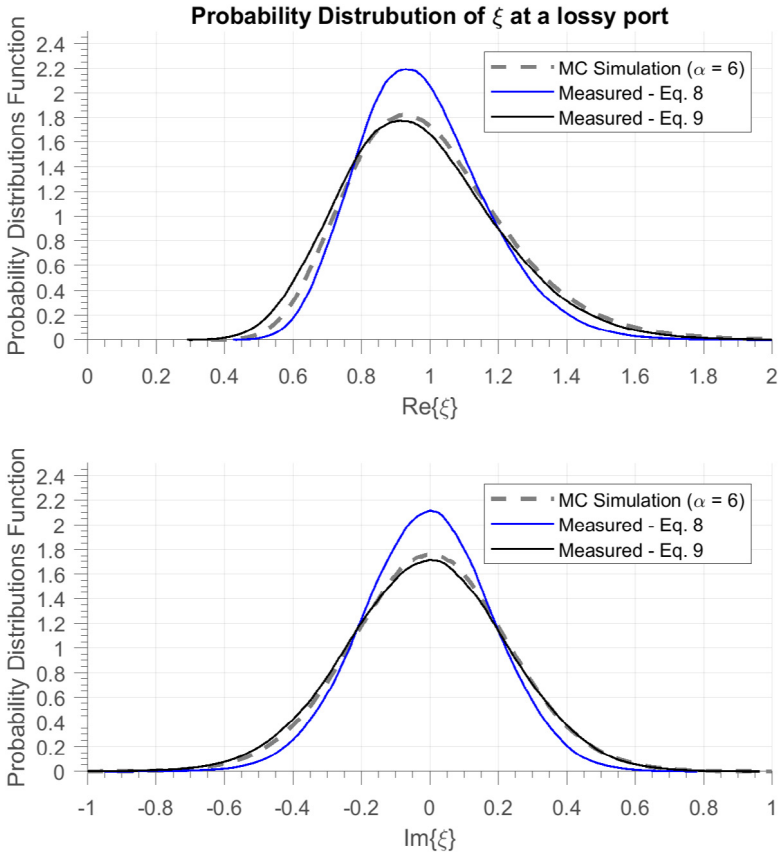

Fig. 7. A comparison of the pdfs of the real (top) and imaginary (bottom) part of the measured and computed normalized impedances for a lossy port.

can be extracted using the time gating method (TGM). The possible errors in the TGM are discussed in the context of the early implementation of the TGM inside a network analyzer by Lu. et al. [19]. They have grouped them in four categories. The first is the out of gate attenuation error. This occurs if the gating window function is not equal to zero outside the gating window. In which case, it does not completely suppress the unwanted reflections. A rectangular window will avoid this error. However, the sharp edges of the rectangular window in the time domain can cause a ringing effect in the frequency domain. Modern VNAs often use other windowing function to balance the ringing effects while also minimizing the out of gate attenuation error. The second type of error is truncation error. This arises when there is an overlap in time between the desired signal and the signal we want to suppress. By suppressing the unwanted segment in time, we are also losing the tail of the signal of interest. This is important to keep in mind when deciding on the gating time. The third and fourth types of error are masking error and multi-reflection aliasing error. Both of which arise when we want to suppress the prompt reflection and keep the subsequent reflections. Therefore, it does not apply in this context.

Finally, the measurements of the radiation impedance assume negligible power loss at the port. This means the incident power at the antenna is either promptly reflected or radiated into the cavity. Conversely, if the power is lost locally at the port due to a lossy antenna, the radiation impedance cannot be directly measured with TGM or any of the methods previously discussed. This situation is addressed by the authors of Ref. [20]. The result in the high loss limit ($\alpha \gg 1$) is a new formulation of the RCM that includes the radiation efficiency (η) of the antenna. Updating Eq. (11) for the normalized impedance we find

$$\xi_m = \frac{Z_{cav} - j\bar{X}}{\eta \bar{R}} + \frac{(\eta - 1)}{\eta} \tag{12}$$

For example, we can consider a lossy antenna in the aluminum cavity discussed in Section 3. A copper trace on FR4 circuit board forms a loop antenna that has some localized power loss in the frequency range of 3 GHz - 3.5 GHz. The antenna is simulated in ANSYS HFSS [21] from which the radiation efficiency can be computed. The radiation efficiency over this frequency fluctuates between 0.69 and 0.81 for an average of 0.75. Others have shown methods to experimentally measure the radiation efficiency [22]. Using the computed value of η, we normalize the impedance by applying Eq. (12). In Fig. 7, very good agreement is shown between the data normalized according to Eq. (12) with the prediction distribution of ξ computed for the measured loss parameter ($\alpha = 6$). Conversely, if we had assumed that the port had negligible loss and applied Eq. (11), the variance of the normalized impedance would be smaller due to the unaccounted-for port loss.

Please cite this article in press as: B. Addissie, et al., Extraction of the coupling impedance in overmoded cavities, Wave Motion (2018), https://doi.org/10.1016/j.wavemoti.2018.09.011.

6. Conclusion

In this paper, we presented a new way to measure the average impedance, to be used in the random coupling model (RCM), using the time gating method (TGM). The method allows for determination of the average impedance in situ, without the need to modify the configuration or to make a separate measurement. By increasing the gating time, the TGM is shown to have the capability of including the effects of reflections of increasing time delay in determining the average impedance. Consequently, increasing the time delay gives a frequency dependent impedance with finer resolution. Additionally, the effect of antenna losses can be treated by including the antenna's radiation efficiency. However, this requires an additional measurement. The method has been experimentally demonstrated and produces values for the average impedance about which there are fluctuations of impedance with distributions in agreement with the RCM.

Acknowledgments

This work is partially supported by the AFOSR/AFRL Center of Excellence: The Science of Electronics in Extreme Electromagnetic Environments, United States FA95501510171, and the Office of Naval Research, United States under N000141512134.

References

[1] Richard Holland, Statistical Electromagnetics, first ed, CRC Press, 1999.
[2] L.K. Warne, K.S.H. Lee, H.G. Hudson, W.A. Johnson, R.E. Jorgenson, S.L. Stronach, Statistical properties of linear antenna impedance in an electrically large cavity, IEEE Trans. Antennas and Propagation 51 (5) (2003) 978–992.
[3] Xing Zheng, Thomas M. Antonsen Jr, Edward Ott, Statistics of impedance and scattering matrices in chaotic microwave cavities: Single channel case, Electromagnetics 26 (1) (2006) 3–35.
[4] Xing Zheng, Thomas M. Antonsen, Edward Ott, Statistics of impedance and scattering matrices of chaotic microwave cavities with multiple ports, Electromagnetics 26 (1) (2006) 37–55.
[5] Sameer Hemmady, Xing Zheng, Edward Ott, Thomas M. Antonsen, Steven M. Anlage, Universal impedance fluctuations in wave chaotic systems, Phys. Rev. Lett. 94 (2005) 014102.
[6] S. Hemmady, T.M. Antonsen, E. Ott, S.M. Anlage, Statistical prediction and measurement of induced voltages on components within complicated enclosures: A wave-chaotic approach, IEEE Trans. Electromagn. Compat. 54 (4) (2012) 758–771.
[7] Gabriele Gradoni, Jen-Hao Yeh, Bo Xiao, Thomas M. Antonsen, Steven M. Anlage, Edward Ott, Predicting the statistics of wave transport through chaotic cavities by the random coupling model: A review and recent progress, Wave Motion 51 (4) (2014) 606–621, Innovations in Wave Modelling.
[8] P.W. Brouwer, C.W.J. Beenakker, Voltage-probe and imaginary-potential models for dephasing in a chaotic quantum dot, Phys. Rev. B 55 (1997) 4695–4702.
[9] C.W.J. Beenakker, Random-matrix theory of quantum transport, Rev. Modern Phys. 69 (1997) 731–808.
[10] Y. Alhassid, The statistical theory of quantum dots, Rev. Modern Phys. 72 (2000) 895–968.
[11] M.L. Mehta, Random Matrices, in: Pure and Applied Mathematics, vol. 142, Elsevier Science Limited, 2004.
[12] G. Burrell, A. Jamieson, Antenna radiation pattern measurement using time-to-frequency transformation (tft) techniques, IEEE Trans. Antennas and Propagation 21 (5) (1973) 702–704.
[13] P. Gonzlez-Blanco, M. Sierra-Castaer, Time filtering techniques for echo reduction in antenna measurements, in: 2016 10th European Conference on Antennas and Propagation (EuCAP), 2016, pp. 1–3.
[14] J. Tian, L. Zhang, N. Li, W. Chen, Time-gating method for v/uhf antenna pattern measurement inside an anechoic chamber, in: 2008 International Conference on Microwave and Millimeter Wave Technology, Vol. 2, 2008, pp. 942–945.
[15] Q. Xu, Y. Huang, L. Xing, Z. Tian, M. Stanley, S. Yuan, B-Scan in a reverberation chamber, IEEE Trans. Antennas and Propagation 64 (5) (2016) 1740–1750.
[16] Jen-Hao Yeh, James A. Hart, Elliott Bradshaw, Thomas M. Antonsen, Edward Ott, Steven M. Anlage, Universal and nonuniversal properties of wave-chaotic scattering systems, Phys. Rev. E 81 (2010) 025201.
[17] J.A. Hart, T.M. Antonsen, E. Ott, Effect of short ray trajectories on the scattering statistics of wave chaotic systems, Phys. Rev. E 80 (2009) 041109.
[18] S. Deus, P.M. Koch, L. Sirko, Statistical properties of the eigenfrequency distribution of three-dimensional microwave cavities, Phys. Rev. E 52 (1995) 1146–1155.
[19] K. Lu, T.J. Brazil, A systematic error analysis of hp 8510 time-domain gating techniques with experimental verification, in: 1993 IEEE MTT-S International Microwave Symposium Digest, Vol. 3, 1993, pp. 1259–1262.
[20] B.D. Addissie, J.C. Rodgers, T.M. Antonsen, Application of the random coupling model to lossy ports in complex enclosures, in: 2015 IEEE Metrology for Aerospace (MetroAeroSpace), 2015, pp. 214–219.
[21] Ansoft. ANSYS HFSS, 3D Full-wave Electromagnetic Field Simulation.
[22] C.L. Holloway, H.A. Shah, R.J. Pirkl, W.F. Young, D.A. Hill, J. Ladbury, Reverberation chamber techniques for determining the radiation and total efficiency of antennas, IEEE Trans. Antennas and Propagation 60 (4) (2012) 1758–1770.